Development of tantalum scaffold for orthopaedic applications produced by space-holder method

E. Rupérez*[1,3], J.M. Manero[1,2,3], K. Riccardi [1,2], Yuping Li[4], C. Aparicio[4] and F. J. Gil[1,2,3]

[1] Biomaterials, Biomechanics and Tissue Engineering Group, Department of Materials Science and Metallurgical Engineering (UPC), ETSEIB, Av. Diagonal, 647, 08028 Barcelona, Spain

[2] Biomedical Research Networking Centre in Bioengineering, Biomaterials and Nanomedicine (CIBER-BBN), Campus Río Ebro, 50018 Zaragoza, Spain

[3] Centre for Research in NanoEngineering (CRNE), (UPC), C/Pascual i Vila 15, 08028 Barcelona, Spain

[4] Minnesota Dental Research Center for Biomaterials and Biomechanics, University of Minnesota School of Dentistry, 515 Delaware St. SE, Minneapolis, MN, 55455, USA

***Corrresponding Author:**

Elisa Rupérez, PhD
Department of Materials Science and Metallurgical Engineering (ETSEIB)
Technical University of Catalonia (UPC)
Av. Diagonal, 647, Barcelona, 08028, Spain.
Tel: (+34) 934010714
Fax:+34 934016706
E-mail: elisa.ruperez@upc.edu

Abstract

In the present study, production of tantalum porous scaffolds using the space holder technique was performed. The effect of size and content of sodium chloride particles, used as space holder, as well as compacting pressure on foam structure and mechanical properties have been investigated. The morphological characterization was carried out by means of scanning electron microscopy (SEM), mercury intrusion porosimetry (MIP) and micro-CT technique. The relationship between the elastic modulus and yield strength of the tantalum porous scaffold and the pore structure was evaluated. Space holder technique allows obtaining tantalum open-cell structure (70 % of porosity) and modulus of elasticity similar to cancellous bone, with reproducible processability into three-dimensional structures and reasonable manufacturing costs.

Keywords: Porous Tantalum, tissue engineering, space holder method, powder metallurgy

1. Introduction

General population still faces significant increase of bone and musculoskeletal problems, which consequently produces an increasing demand for long term clinical performance of a bone replacement implant (Kurtz et al., 2007). Usually, for bone tissue engineering, grafting materials are designed with porous structures to facilitate space for bone in-growth and vascularisation (Bobyn et al., 1999; Hernández et al., 2002; Ayers et al., 2000). The high porosity and its interconnected structure facilitate transport of body fluids, benefit the spread of cells into the implant, and promote proliferation of bone tissue by increasing the contact area (Bansiddhi et al., 2008; Karageorgiou and Kaplan, 2005). In the literature, different materials such as ceramics (Galois and Mainard, 2004), polymers (Liu and Ma, 2004; Wua et al., 2014) or metallic scaffolds (Jung el al., 2015; Wielding et al., 2015) have been proposed as porous implants to be used in bone tissue engineering. Ceramics or polymer scaffolds have been studied showing promising bioactive features; however, the low strength of polymers as well as brittleness of ceramics are notable drawbacks for bone implant applications.

Currently, metallic scaffolds are the most suitable materials for load-bearing implants due to their mechanical properties: the elastic modulus similar to bone minimizes the stress-shielding effect (Wua et al., 2014) with high fracture toughness and load impact fractures. For that reason, numerous surface coatings and porous designs of commercially pure titanium, Ti6Al4V or NiTi foams have been developed to improve biological fixation in the orthopedic field (Wang et al., 2009; Mediaswanti et al., 2013; Hosseini et al., 2014). Although good clinical results have been shown with these materials, they have several drawbacks (possible release of toxic ions, low osteoconductivity or low frictional characteristics). Further, a metallic scaffold will not form sufficiently strong chemical bonds with bone tissue and thus, „loosening‟ of the implant over a long period may become a critical problem (Kim et al., 1996; Spoerke and Stupp, 2005). To overcome

these limitations, tantalum has been proposed as a new material for designing porous metallic grafts (Balla et al., 2010a, Koutsostathis et al., 2009). Tests in vivo had demonstrated no dissolution of the tantalum metal after several weeks of implantation and inflammatory reactions in the tissues surrounding tantalum implants were not evident (Matsuno et al., 2001).

Tantalum, a metal of noteworthy interest for biomedical applications, especially in orthopaedic and dentistry, has high strength, ductility and corrosion resistance with excellent biocompatibility (Kato et al., 2000; Maccauro et al., 2009). Moreover, tantalum forms a self-passivating surface oxide layer that leads to the formation of a bone-like apatite coating in vivo. This surface allowed excellent bone and fibrous in-growth properties that led to a rapid and substantial bone and soft tissue attachment (Levine et al., 2006; Fernández-Fairén et al., 2012).

The historical and current use of tantalum in pacemaker electrodes, plates for cranioplasty, femoral stems or plates in nerve surgery, makes this material a good candidate for a wide variety of implants (Bobyn et al., 1999). Furthermore, studies “in vitro”, showed six times higher living cell density, excellent cellular adherence and growth with abundant extracellular matrix formation on Ta surfaces than on Ti surfaces (Balla et al., 2010b). Jafari SM et al. (2010) demonstrated that tantalum cups presented better results than titanium cups in clinical cases presented with severe bone deficiency. Therefore, tantalum is gaining attention and has been proposed for designing new porous metallic grafts (Ryan et al., 2006).

Nevertheless, the use of tantalum has been limited because of its high cost and difficult processing as it has a high melting point and high affinity for oxygen. Its high density is also a drawback which has prevented a larger development of Ta implants. Thus, several studies are now focusing either on tantalum thin film formation on other commonly used

metallic implants or tantalum porous scaffolds development (Lewis, 2013; Maho et al., 2012; Zardiackas et al., 2001).

Metallic scaffolds can be produced in a variety of ways; the choice of the technique depends on the requirements of the final application (Ryan et al., 2006). The basic goal of the available manufacturing techniques is to produce a micro-architecture in a scaffold that is highly porous to allow for cell adhesion, vascularization, nutrient flow and appropriate mechanical properties (Lewis, 2013)

Different methods for the fabrication of metallic scaffolds have been reported including conventional techniques such as sintered metal powders, space holder method, gas foaming; and advanced technologies like spark plasma sintering, laser-engineered net-shaping process (LENS) (Kato et al., 2000; Bandyopadhyay et al., 2009; Balla et al., 2009) , selective laser sintering (SLS), electron beam melting (EBM), Direct Laser Processing (Balla et al., 2010b), and spark-plasma-sintering (SPS) (Angerer et al, 2007).

One technique successfully used for manufacturing open-cell porous tantalum structures is chemical vapor deposition (CVD)/injection (CVI) on an interconnected vitreous carbon skeleton. These structures are characterized by a volume porosity of roughly 75–85%, a pore size ranging from 400 to 600 μm and with sufficient strength to allow physiological load-carrying applications (Bobyn et al., Zardiackas et al., 2001, Sevilla et al., 2007). Considering that its high cost is one of the main drawbacks of this technique, the “space holder method” has been selected in this work as an alternative method to produce non-homogenous porous tantalum samples with an open cell structure.

Several review articles on scaffold materials and fabrication technologies highlight the space holder method as one of the effective methods for the fabrication of metallic biomedical scaffolds, owing to its ability to produce a wide range of porosity levels and controllable pore geometry in scaffolds (Sing et al., 2010; Banhart, 2001). Type, size and morphology of the space-holding particles determine the porous structure and mechanical

properties of the manufactured structure (Arifvianto and Zhou, 2014). A number of space holder materials have been used such as carbamide ($CO(NH_2)_2$) (Wenjuan et al., 2009), ammonium hydrogen carbonate (NH_4HCO_3) and sodium chloride (NaCl) (Ye and Dunand, 2010; Bansiddhi and Dunand, 2008; Wen et al., 2002).

Even though there is prolific literature on the use of this method to produce porous structures of titanium and titanium alloys (Torres et al., 2012; Pflüger et al., 1980), there have been only limited attempts to apply it to produce tantalum structures (Zhou and Zhu, 2013). The purpose of this work is to analyze the effects of porosity, size of NaCl holding-space particles, and compaction pressure on the morphological and mechanical properties of open cell tantalum structures produced using the space holder technique.

2. Materials and methods

2.1. Sample preparation

Scaffold fabrication with the space holder method relies on temporary particles added to metallic matrix powder (space holding particles) that act as a pore former. **Figure 1** schematically shows that four processing steps are involved: mixing of metal matrix powder and space-holding particles, compaction of powders materials, removal of space-holding particles and sintering of porous green compact. The process has been described on a recent patent developed by our research group (Rupérez et al., 2012).

As a space holder, sodium chloride particles have been selected in order to minimize undesirable reactions between matrix powder (Ta) and space-holding particles as well as for their biocompatibility and non-cytotoxicity properties.

Elemental metal powders of Ta (Alfa Aesar, Puratronic 99,97%) and particles of NaCl (Panreac Química S.A.U., Spain, purity > 99.5) were weighed to get a porosity of 60-80% vol. For a given porosity and from tantalum and sodium chloride density (ρ_{Ta} and ρ_{NaCl}

respectively), the mass of each component (m_{Ta}, m_{NaCl}) required to make the blends was calculated according to Equation [1]:

$$\%\text{vol. Porosity} = \frac{{}^{m_{NaCl}}/_{\rho_{NaCl}}}{{}^{m_{NaCl}}/_{\rho_{NaCl}} + {}^{m_{Ta}}/_{\rho_{Ta}}} \times 100 \qquad [1]$$

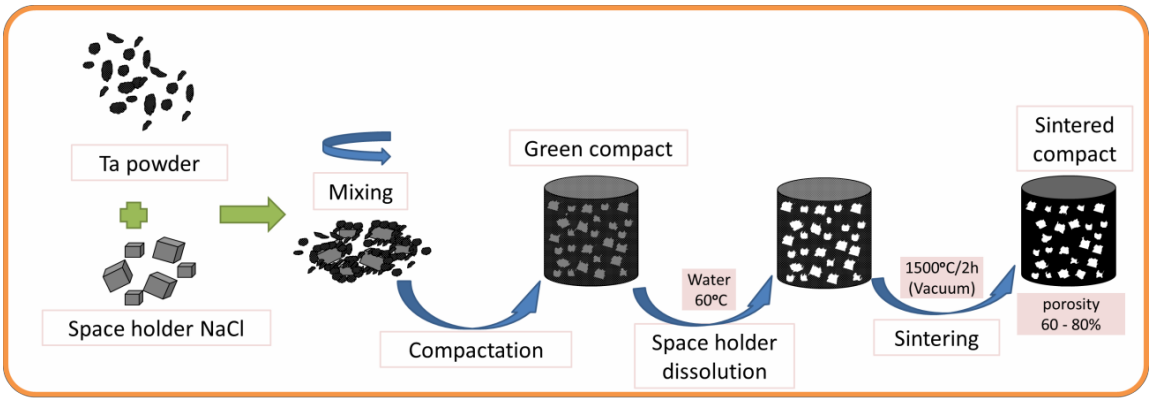

Figure 1 Outline of space-holder process

In this paper we have evaluated morphological and mechanical properties of tantalum porous structures with 60, 70 and 80% of porosity and compacted at 350 and 450 MPa. Given that size of space-holder particles will define the final pore size, the degree of pore interconnectivity and thus the final mechanical properties of the Ta scaffold, two NaCl particles size ranges were studied (S, small:100-397μm and L, large: 397-940μm). Three space holder blends were tested: 100% of large particles (0:100), 50% of small and big size particles respectively (50:50) and samples with higher percentages of smaller size particles (70:30). **Table 1** shows the different test conditions that were performed.

The mixing of Ta powder and NaCl particles was carried out with a mixer (SPEX SamplePrep 8000-series) using ethanol as a binder. Subsequently, uniaxial die compaction was performed with the aid of a pair of punches that moved uniaxially through a die filled with granular materials using a servo-hydraulic testing machine (MTS-Bionix, USA).

Cylindrical specimens were compacted to 7mm in diameter and 9 mm in length at two compaction pressures of 350 MPa and 450 MPa.

Table 1. Volume fraction of space-holding particles with range sizes studied. (S:100-397μm and L: 397-940μm).

Sample Ref.	%vol. NaCl	Particle size NaCl (%) ratio S (100-397)μm: L (397-940)μm
60$_{(0:100)}$	60	0:100
60$_{(50:50)}$	60	50:50
60$_{(70:30)}$	60	70:30
70$_{(0:100)}$	70	0:100
70$_{(50:50)}$	70	50:50
70$_{(70:30)}$	70	70:30
80$_{(0:100)}$	80	0:100
80$_{(50:50)}$	80	50:50
80$_{(70:30)}$	80	70:30

In order to ensure a complete removal of space-holding particles and a quick dissolution process, water at 60ºC was chosen as the leaching medium. As any reaction between decomposed space-holding particles and the scaffold framework material may negatively impact on the mechanical properties of the scaffold, the total NaCl dissolution was assessed by means of electric conductivity measurements of the waste water.

The sintering process was performed at 1500ºC under vacuum conditions in a tubular furnace (Carbolite, Horizontal vacuum tube furnace) for two hours.

2.2. Structural characterization of the sintered scaffolds

The morphological characterization of tantalum powders and NaCl particles were carried out by means of scanning electron microscopy (SEM; JEOL 6400 JSM). The size distribution, mean size and percentages ratios of NaCl and tantalum particles were characterized by laser diffraction technique (Beckman Coulter LS Particle Size Analyzer).

Porosity of sintered tantalum structures (open cells), the pore size distribution and its isotropy were characterized by means of mercury intrusion porosimetry (MIP, Micromeritics' AutoPore IV 9500), metallographic examination with a scanning electron microscope (JEOL 6400 JSM) and micro-CT.

The three dimensional structure of the sintered Tantalum specimens was determined using a Microcomputed tomographer (µ-CT, HMX-XT 225, X-tek system, United Kingdom) at 190 kV and 330 µA. A total of 720 projections and 4 frames per projection were acquired. The volumetric reconstruction with the microradiographs was performed using the CT Pro 3D (Nikon Metrology, Brighton, MI, USA). The reconstructed volume was then analyzed using VG Studio Max (Version 2.1.3, 64bit, Volume Graphics, Charlotte, NC, USA).

2.3. Mechanical characterization of sintered scaffolds

Compression tests were performed according to ASTM F 451 standard. Five specimens of each material were tested in compression at a cross-head speed of 10 mm/min. Load versus extension was continuously monitored and recorded. These mechanical tests were carried out using a servo-hydraulic testing machine (MTS-Bionix, USA). Assays were performed with cylindrical samples of 7 mm in diameter and 9 mm in length.

3. Results and discussion

3.1 Characterization of tantalum powder and space-holder NaCl particles

SEM micrographs show the morphology of the tantalum matrix powder and the space-holder particles (Fig. 2a and 3a). It is clearly shown that Ta powder presented an irregular shape whereas the NaCl particles had a typical cuboid shape.

Figure 2b, 3b and 3c present the size particles distribution, measured by means of laser diffraction technique, for the raw tantalum powder as well as for the two sieved NaCl samples studied. For the tantalum powder, 95% of the particles had a size smaller than

65.6µm with a mean size of 30.85 ± 18.76µm. In the case of space holder, the mean particle size were 240.5 ± 86.5µm for the S (small) size range and 541.7± 146.4µm for the B (Big) size range.

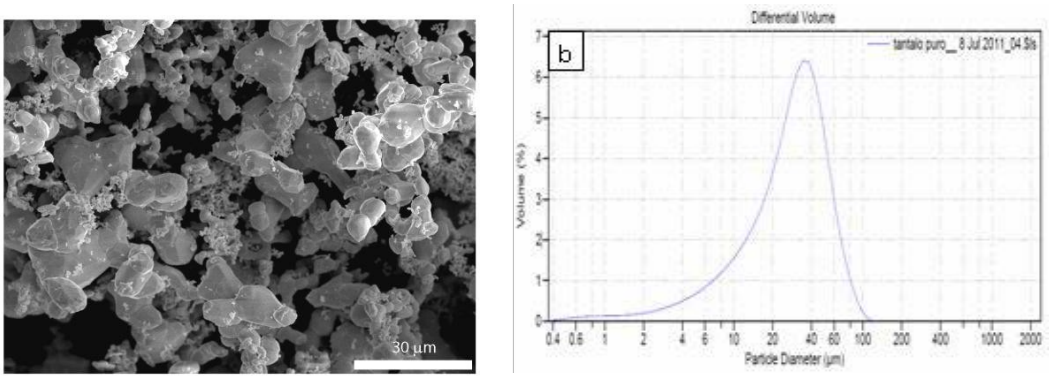

Figure 2 Particles of tantalum powders (Alfa Aesar, Puratronic), a) SEM image and b) Ta particles size distribution analyzed by laser diffraction technique.

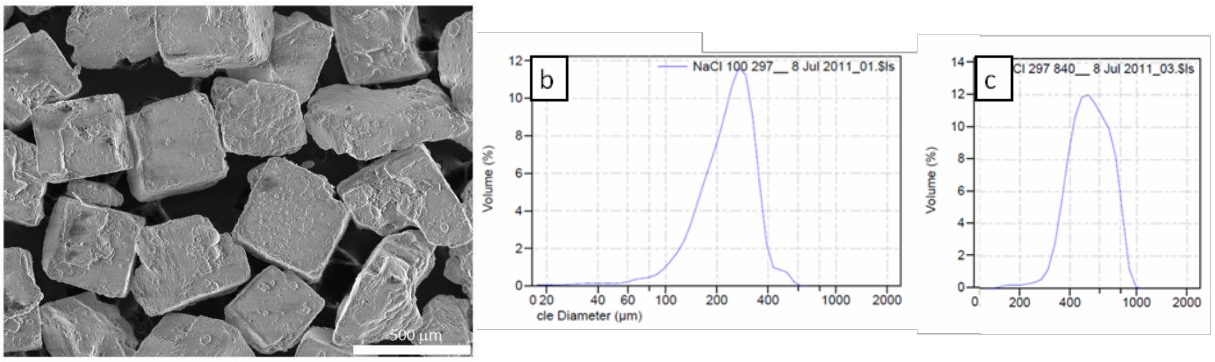

Figure 3 NaCl space holder particles, a) SEM image, b) and c) particles size distribution analyzed by laser diffraction technique in range 100-397 µm and 397-940 µm respectively.

The properties of a sintered scaffold and its densification during sintering depend on the sizes of the matrix powder particles (Arifvianto and Zhou, 2014). Unfortunately, there are no data available about the optimal size range and morphology of Ta powder for the production of scaffolds. Nevertheless, for titanium foams, it is reported that angular matrix powder particles led to a higher green strength of compact (Tuncer et al., 2011) keeping its structure during the removal of space-holding particles and provide higher porosity and larger pore sizes than spherical powder particles (Álvarez and Nakajima, 2009). Previous

studies for Ta scaffolds have shown that tantalum powders having sizes bigger than 20 μm resulted in scaffold frameworks with voids and sintering necks (Rupérez et al., 2012).

3.2.- Microstructural characterization of sintered tantalum scaffolds

One of the main problems of the space holder method could be the insufficient green strength of the samples after removal of the NaCl particles. Open cell structures with porosity greater than 75% should be handled with care in order to avoid the risk of damaging its structural integrity.

Figure 4 shows a porous tantalum cylinder compacted at 350 MPa and sintered at 1.500ºC with 70% of porosity. An interconnected porous structure with good integrity is clearly shown.

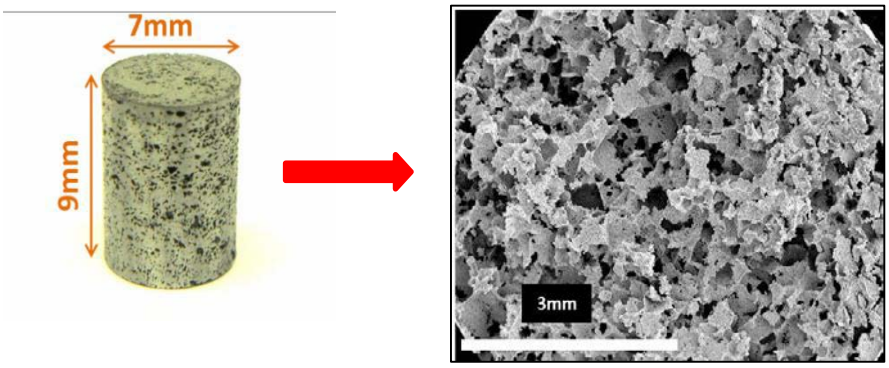

Figure 4 Sintered porous tantalum cylinder with 70% of porosity, compacted at 350 MPa and sintered at 1.500ºC.

The percentage of interconnected macro-pores and the mean interconnected size (μm) were carried out by means of MIP technique in all cases (**Tables 2-4**). The results showed that samples with theoretical porosity of 60% presented lower values of porosity, particularly when larger particle sizes were used (0:100). In this case, the experimental porosity values ranged between 35-62 %.

Table 2 Porosity and pore size entrance in foams with 60% vol. space holder measured by MIP technique.

Sample Ref.	Compactation pressure (MPa)	Open Porosity %	Pore size entrance (µm)
$60_{(0:100)}$	350	35.0 ± 2.1	43.56 ± 4.07
	450	38,6 ± 3.7	40,03 ± 4.81
$60_{(50:50)}$	350	55,7 ± 5.6	44,98 ± 3.13
	450	61,8 ± 4.3	44,99 ± 2.86
$60_{(70:30)}$	350	52,2 ± 3.7	44,99 ± 4.77
	450	55.8 ± 2.6	51,37 ± 3.92

Table 3 Porosity and pore size entrance in foams with 70% vol. space holder measured by MIP technique.

Sample Ref.	Compactation pressure (MPa)	Open Porosity %	Pore size entrance (µm)
$70_{(0:100)}$	350	62,4 ± 2.4	89 ± 6.05
	450	63,7 ± 1.8	87,2 ± 5.96
$70_{(50:50)}$	350	71,0 ± 2.4	76,05 ± 5.41
	450	68,9 ± 3.6	76,18 ± 3.18
$70_{(70:30)}$	350	70,2 ± 2,0	60,32 ± 4.89
	450	71,4 ± 1.7	51,36 ± 6.34

Table 4 Porosity and pore size entrance in foams with 80% vol. space holder measured by MIP technique.

.

Sample Ref.	Compactation pressure (MPa)	Open Porosity %	Pore size entrance (µm)
$80_{(0:100)}$	350	78,0 ± 1.5	103,23 ± 10.92
	450	78,4 ± 2.0	120,01 ± 12.08
$80_{(50:50)}$	350	79,0 ± 3.1	76,02 ± 5.97
	450	82,6 ± 2.2	79 ± 4.71
$80_{(70:30)}$	350	81,2 ± 2.5	69 ± 6.04
	450	81,0 ± 1.9	75,91 ± 7,23

Considering that the initial ratios Ta/NaCl mixtures, prior to compaction, were correct (confirmed by laser diffraction analysis) and that the MIP technique is restricted to

measuring the interconnected porosity on the cylinder surface, it could be assumed that part of the pores are not interconnected (close cells). If so, the close cells are most likely located in the core of the porous sample. For samples with low porosity, using bigger size particles leads to a higher probability to find isolated particles leading to structures with lower interconnected porosity.

Furthermore, it is observed that the pore size entrance is, practically, independent of the compaction pressure used (350 and 450MPa). Probably, this is valid as long as the compaction pressures used cannot break the NaCl particles. Regarding the effect of NaCl particle size, the pore size entrance increases when the NaCl particles are bigger (see tables 3 and 4, i.e 0:100). This makes sense because if the particle size is greater, the contact area between them will be bigger leading to a greater pore size entrance. This is valid for the porosities range between 70 and 80%, in which all the porosity is, practically, open. However, for lower porosity (Table 2), this relationship is not clear, probably, due to there are isolated pores not interconnected.

It is possible to obtain porosities slightly higher than the theoretical values. In the theoretical calculation of the weights of tantalum and NaCl necessary to achieve a given porosity, it has not been taken into account the microporosity present between tantalum particles after the sintering process. Moreover, for the sintering temperature used (1.500ºC), the shrinkage is small, approximately, less than 3%.

The analysis of Ta porous samples by SEM **(Figure 5)** corroborated the MIP results as they showed some non-interconnected pores in samples with porosities lower than 60% (Figure 5a-b). However, results from samples $70_{(50:50)}$, $70_{(70:30)}$, $80_{(0:100)}$, $80_{(50:50)}$ and $80_{(70:30)}$) show mainly interconnected pores as the measured porosity corresponded to the percentage of NaCl particles used, that is, the theoretical values of porosity (**Tables 2-4**). Nevertheless, for bigger size NaCl particles ($70_{(0:100)}$), the presence of a small proportion of closed pores inside the scaffold led to a slight decrease of porosity measured by MIP.

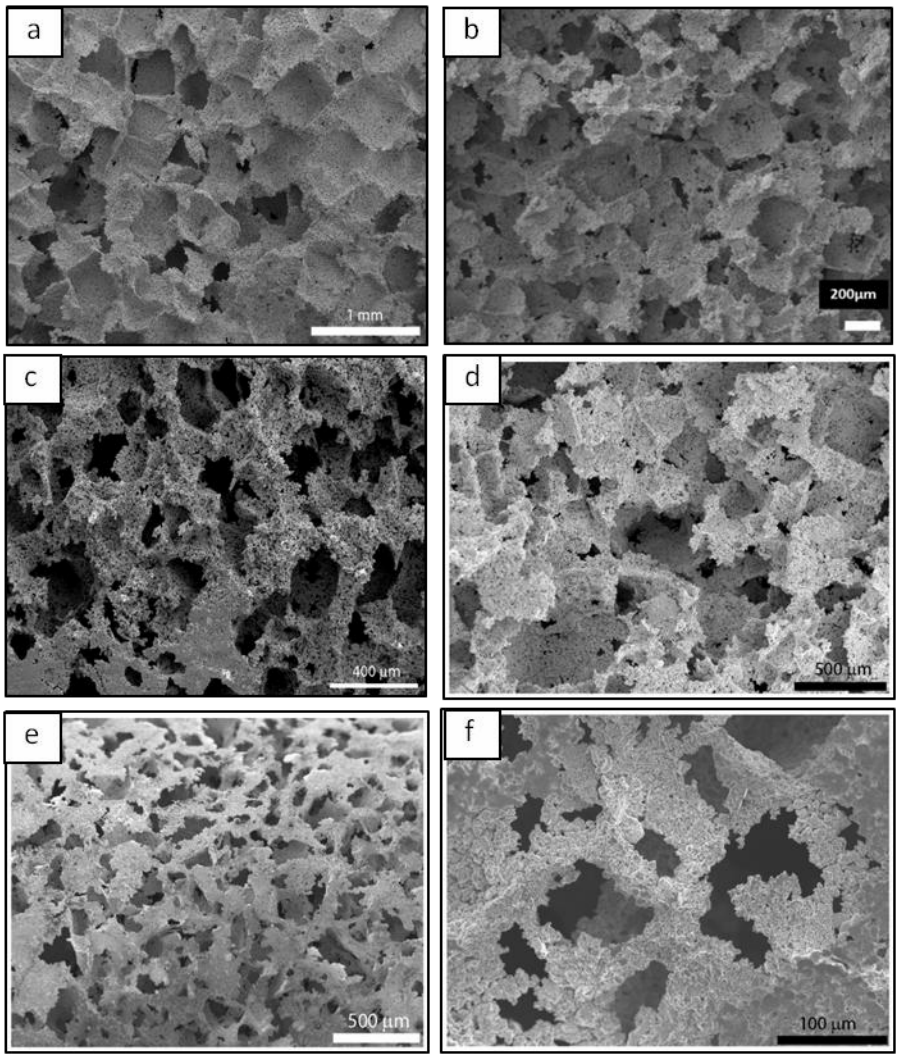

Figure 5 Porous structure of a cross section of cylindrical Ta samples: a) and b) 60% porosity, c) and d) 70% porosity, e) and f) 80% porosity

The μ-CT images of the sintered Ta scaffolds also demonstrated that the porosity among the different groups was mostly, if not completely, interconnected (attached video). This is better visualized on the the extrated porous stuctures (yellow colored images); i.e., the negative images of the reconstructed structures (Figure 6).

It appears that the space holder method was suitable for producing open-cell structures above 70%vol. of porosity, according to all these experimental results. The experimental values of porosity were in agreement with the theoretical values calculated with equation [1] and thus,contraction was hardly observed in the sintered samples. Moreover, the use of mixtures of NaCl with smaller particle size promoted the formation of interconnected

pores for samples with low porosity, as for example in $60_{(50:50)}$. In all cases, the of macro-pore interconnected size increased when the space-holding particle sizes were larger, in accordance with Arifvianto and Zhou (2014).

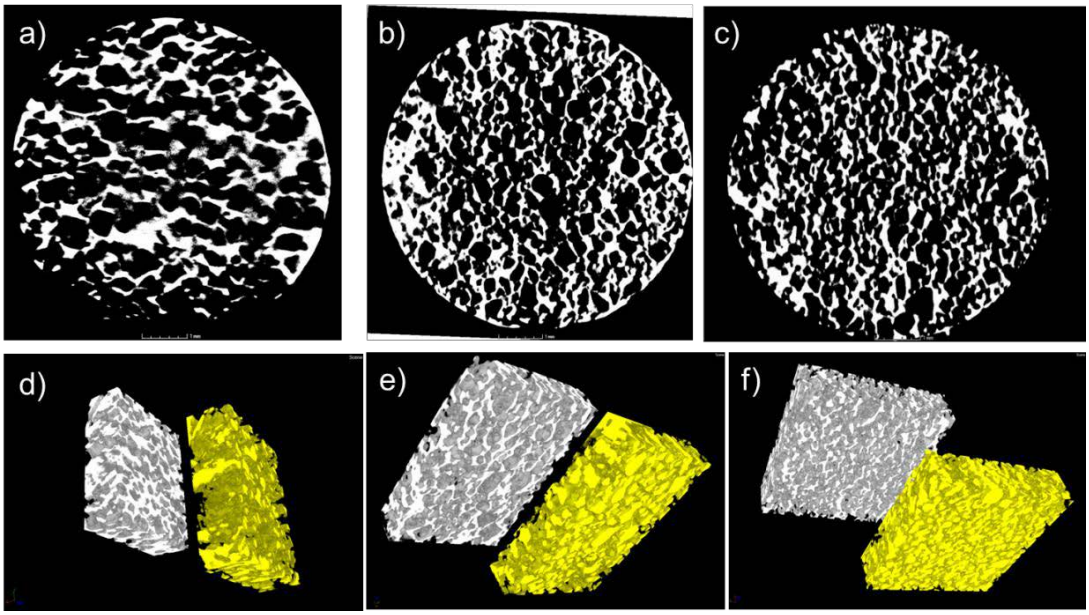

Figure 6. Micro-tomographic images of sintered Ta (70% of porosity). a) and d) 0:100, b) and e) 50:50, c) and f) 70:30. 3D images in yellow color are the porous structures extracted (negative image) from the corresponding Ta scaffolds (gray).

It is well known that open pores are built up from coalesced space-holding particles as a consequence of the compaction process, while closed pores are formed from isolated space-holding particles in the mixture. This study revealed that the transition from closed or isolated pores to interconnected pores occurred when the total porosity of the scaffolds reached 70%.

3.3.- Mechanical characterization of sintered tantalum scaffolds.

The elastic modulus and the yield strength of sintered samples in terms of porosity, space holder size distribution and pressure compaction were assessed by compression tests. From the graphs obtained the behavior of Tantalum porous structures in the elastic region

might be highlighted. **Figure 7** shows the stress-strain curve of a $60_{(0:100)}$ sample compacted at 350 MPa.

As shown in the graph for stresses below the yield strength, an increase in the slope occured. This behavior was observed for most of the tested specimens. The change in Young‟s modulus with the increasing applied stress was probably due to the heterogeneity in the pore distribution of the scaffold. Others have described this same response in tensile tests of open cell nickel and copper foams (Ochiai et al., 2010). Ashby emphasized in *Metal Foam: A Design Guide* (Ashby et al., 2000) that the slope of the initial loading stress-strain graph of metal foams in uniaxial tension and compression tests is lower than that of the unloading curve. Thus, it is more accurate measuring the Young modulus when the specimen is unloaded just before the stress reaches the yield strength.

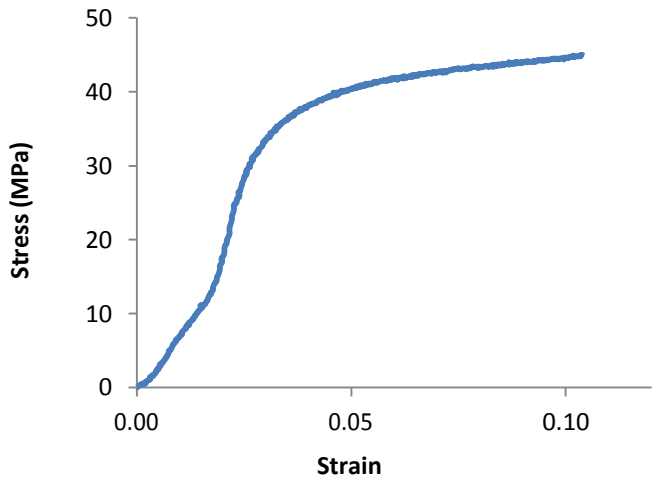

Figure 7 Stress-strain curve of compression test for a Ta sample with 60% porosity, large NaCl particles (0:100) and compaction at 350 MPa.

Due to the porous structures heterogeneity characteristics of the space-holder method, it‟s probably that the increase in the slope may be a consequence of the local plastic deformation within the cell walls and local densification of porous structures blocks at high strain levels.

Figure 8 shows the relationship between Young´s modulus and yield stress values versus the final porosity of the Ta scaffolds. Not surprinsingly, the stiffness and compressive strength of these porous structures decreased with increasing porosity. The Young modulus values of tested samples with 60% porosity were 1.5 - 2.3 GPa, those with 70% porosity were 0.8 - 1.1 GPa and for those with 80% porosity were close to 0.35 GPa.

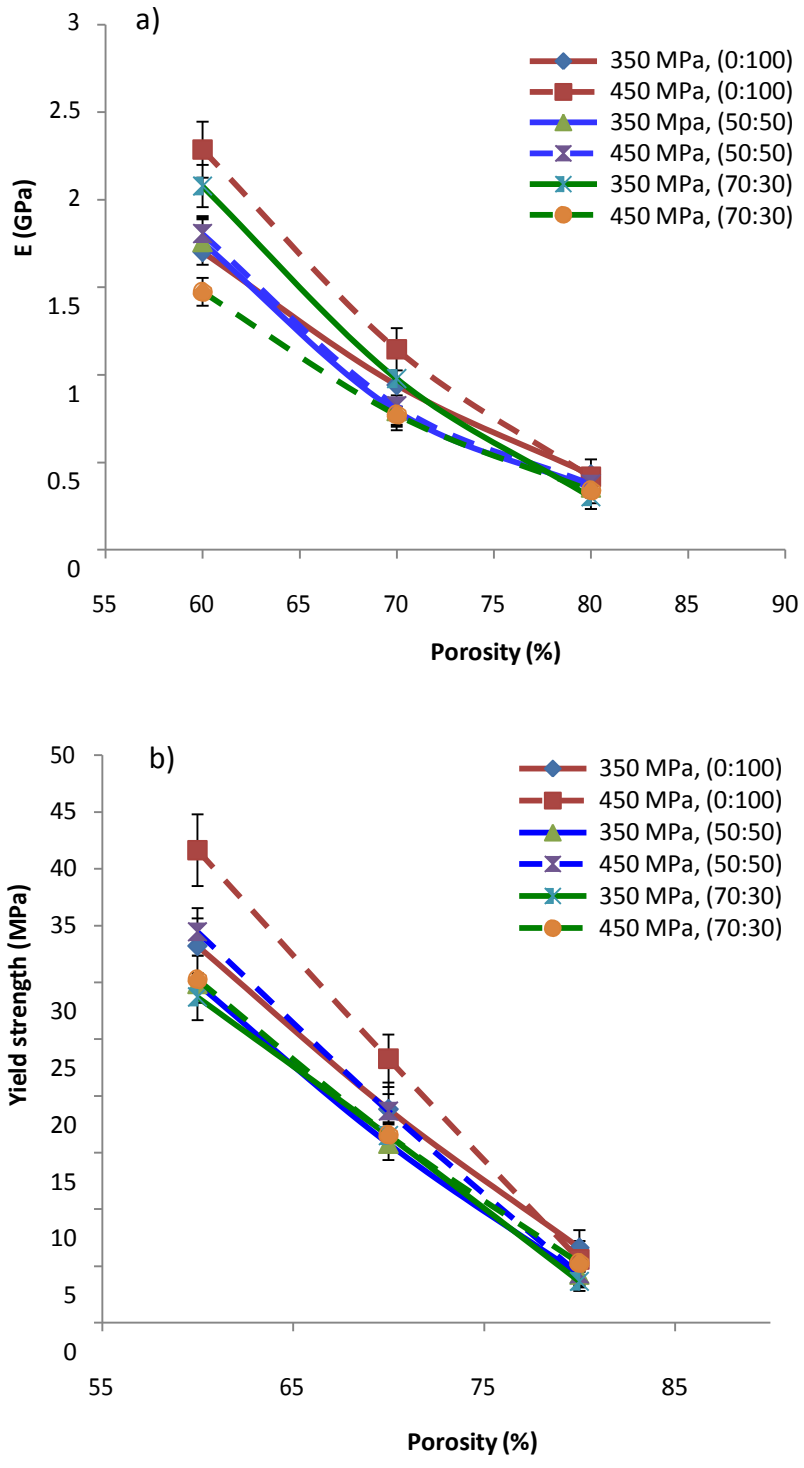

Figure 8 Relationship between the (a) elastic modulus and (b) yield strength versus theoretical porosity.

According to data reported in the literature about values of strength and elastic modulus in compression test of human cancellous bone from two different locations (6.6 to 36.2 MPa and 0.130 to 1.080 GPa, respectively), tantalum open-porous structures developed by space holder method could be suited for their use as substitutes for human bone tissues (Kopperdahl et al., 2002; Goldstein, 1987; Keaveny et al., 1997; Martens et al., 1983).

The yield strength values obtained are higher to those of trabecular bone, and therefore, suitable for bone tissue engineering (Wang X et al., 2010). It is observed that a higher degree of interconnected pores produces a decrease of the corresponding yield strength values, probably, due to a higher pore collapse during the compression test.

The effect of particle size (i.e., pore size) and compactation pressure on the stiffness of the scaffolds (Figure 8a) was less prominent at high porosity. In fact, this effect was almost negligible for a scaffold porosity of 80%. The same response was observed for its influence in the yield strength of the scaffolds (Fig. 8b).

It is worth noting that for samples with 60% porosity, the presence of entrapped NaCl particles in the closed pores that could not be removed by dissolution could have had an influence on the results of the compression tests. As aforementioned this ocurrence caused deviation from the designed values of the scaffold porosity as well as heterogeneity in their mechanical properties.

The compacting pressure had a most notable effect on mechanical properties of the scaffolds for those produced with larger size of space holder particles. The highest values for both yield strength and stiffness of the compacted samples were obtained with a compaction pressure of 450 MPa.

Previous studies have already discussed the relationship between mechanical properties and pore size (Cao et al, 2006; Guden et al., 2008). Results obtained in this work showed that samples processed with larger space holder particles (0:100) produced scaffolds with the highest values of modulus and yield strength.

4. Conclusions

The space holder process used to produce Ta scaffolds allowed the manufacturing of samples with a wide range of porosity levels and controllable pore geometry. This method is a promising candidate for the fabrication of tantalum porous materials in a variety of orthopaedic surgical applications. This yields a simple and cost-effective method for producing high-quality interconnected porous metals.

This study revealed that the transition from closed or isolated pores to interconnected pores occurred when the total porosity of the scaffolds reached 70%. However, using NaCl particles with different size ranges the formation of interconnected pores for samples with lower porosities (60%) was possible.

The open-cell structures obtained with 70 % of porosity were characterized by a morphology and elastic modulus similar to that of cancellous bone. Thus, the space-holder is an appropriate and reproducible method to produce three-dimensional tantalum scaffolds with reasonable manufacturing costs.

Acknowledgements

This study was supported by the Ministery of Science and Innovation (MICINN) and the Ministery of Economy and Competitiveness (MINECO) of the Spanish Government (Projects MAT2009-12547).

5. References

Álvarez and Nakajima, 2009 Alvarez, K.; Nakajima, H., 2009. Metallic scaffolds for bone regeneration. Materials 2, 790–832.

Angerer et al., 2007 Angerer P., Neubauer E., Yu L.G., Khor K.A., 2007. Texture and structure evolution of tantalum powder samples during spark-plasma-sintering (SPS) and conventional hot-pressing. Int. J. Refract. Met. Hard Mater. 25, 280–285.

Arifvianto and Zhou, 2014 Arifvianto B. and Zhou J., 2014. Fabrication of Metallic Biomedical Scaffolds with the Space Holder Method: A Review. Materials 7, 3588-3622.

Ashby et al., 2000 Ashby M.F., Evans A.G., Fleck N.A., Gibson L.J., Hutchinson J.W, Wadley H.N.G., 2000. Metal Foams: A Design Guide, Butterworth-Heinemann, Woburn.

Ayers et al., 2000 Ayers R.A., Bateman T.A., Simske S.J., 2000. Porous NiTi as a material for bone engineering, in: Yahia D.L. (Ed.), Shape Memory Implants. Ed. Springer-Verlag, New Yorkpp. 73-88.

Balla et al., 2009 Balla V. K.,, Bose S., Bandyopadhyay A., 2009. Fabrication of Porous NiTi Shape Memory Alloy Structures Using Laser Engineered Net Shaping. J. Biomed. Mater. Res., Part B 89(2), 481-490.

Balla et al., 2010a Balla V. K., Bodhak S., Bose S., Bandyopadhya A., 2010. Porous tantalum structures for bone implants: Fabrication, mechanical and in vitro biological properties. Acta Biomater. 6, 3349–3359.

Balla et al., 2010b Balla V. K., Banerjee S., Bose S. and Bandyopadhyay A., 2010. Direct Laser Processing of Tantalum Coating on Titanium for Bone Replacement Structures, Acta Biomater. 6(6), 2329–2334.

Bandyopadhyay et al., 2009 Bandyopadhyay A., Krishna B. V., Xue W., Bose S., 2009. Application of Laser Engineered Net Shaping (LENS) to manufacture porous and functionally graded structures for load bearing implants, J. Mater. Sci: Mater. Med. 20, S29–S34.

Banhart, 2001 Banhart J., 2001. Manufacture, characterisation and application of cellular metals and metal foams. Prog. Mater. Sci. 46, 559–632.

Bansiddhi et al., 2008a Bansiddhi A., Sargeant T.D., Stupp S.I., Dunand D.C., 2008. Porous NiTi for bone implants: A review. Acta Biomater. 4 (4),,773–782.

Bansiddhi and Dunand, 2008b Bansiddhi A., Dunand D.C., 2008. Shape-memory NiTi foams produced by replication of NaCl space-holders, Acta Biomater. 4, 1996-2007.

Bobyn et al., 1999 Bobyn J.D., Stackpool G.J., Hacking S.A., Tanzer M., Krygier J.J., 1999. Characteristics of bone ingrowth and interface mechanics of a new porous tantalum biomaterial. J. Bone Joint Surg. 81B, 907-914.

Cao et al., 2006 Cao X., Wang Z., Ma H., Zhao L., Yang G., 2006. Effects of cell size on compressive properties of aluminum foam. Trans. Nonferrous Met. Soc. China 16, 351-356.

Fernández-Fairén et al., 2012 Fernández-Fairen M, Murcia A, Iglesias R, Sevilla P, Manero JM, Gil FJ., 2012. Analysis of tantalum implants used for avascular necrosis of the femoral head: a review of five retrieved specimens. J. Appl. Biomater. Funct. Mater. 10(1):29-36.

Galois and Mainard, 2004 Galois, L., Mainard, D., 2004. Bone ingrowth into two porous ceramics with different pore sizes: An experimental study. Acta Orthop. Belg. 70, 598–603.

Goldstein, 1987 Goldstein, S.A., 1987. The mechanical properties of trabecular bone: dependence on anatomic location and function. J. Biomech. 20, 1055-1061.

Guden et al., 2008 Guden M., Celik E., Hizal A., Altindis M., Cetiner S., 2008. Effects of compaction pressure and particle shape on the porosity and compression mechanical properties of sintered Ti6Al4V powder compacts for hard tissue implantation. J. Biomed. Mater. Res. B Appl. Biomater. 85, 547–555.

Hernández et al., 2002 Hernández R., Polizu S., Turenne S., Yahia L‟H, 2002.. Characteristics of porous nickel–titanium alloys for medical applications. Bio-Med. Mater. Eng. 12, 37-45.

Hosseini et al., 2014 Hosseini S.A., Yazdani-Rad R., Kazemzadeh A., 2014. A Comparative Study on the Mechanical Behavior of Porous Titanium and NiTi Produced by a Space Holder Technique. J. Mater. Eng. Perform. 23 (3), 799-808.

Jafari et al., 2010 Jafari S.M., Bender B., Coyle C., Parvizi J., Sharkey P.F., et al., 2010. Do tantalum and titanium cups show similar results in revision hip arthroplasty? Clin. Orthop. Relat. Res. 468, 459-465.

Jung el al.; 2015. Jung H, Jang T., Wang L., Kima H., Kohd Y., Songa J. Novel strategy for mechanically tunable and bioactive metal implants. Biomaterials. Volume 37, January 2015, Pages 49‑61.

Karageorgiou and Kaplan, 2005 Karageorgiou V., Kaplan D., 2005. Porosity of 3D biomaterial scaffolds and osteogenesis. Biomaterials 26 (27), 5474–5491.

Kato et al., 2000 Kato H., Nakamura T., Nishiguchi S., Matsusue Y., Kobayashi M., Miyazaki T., et al., 2000. Bonding of alkali- and heat-treated tantalum implants to bone. J. Biomed. Mater. Res., 53(1) 28–35.

Keaveny et al., 1997 Keaveny T.M., Pinilla T.P., Crawford R.P., et al., 1997. Systematic and random errors im compression testing of trabecular bone, J. Orthop. Res. 15, 101-110.

Kim et al., 1996 Kim H.M., Miyaji F., Kokubo T., Nakamura T., 1996. Preparation of bioactive Ti and its alloys via simple chemical surface treatment. J. Biomed. Mater. Res. 32, 409-417.

Kopperdahl et al., 2002 Kopperdahl D.L., Morgan E.F., Keavney T.M., 2002. Quantitative computed tomography estimates of the mechanical properties of human vertebral trabecular bone. J. Orthop. Res. 20, 801-805.

Koutsostathis et al. 2009 Koutsostathis S. D., Tsakotos G. A. , Papakostas I., Macheras G. A., 2009. Biological processes at bone – porous tantalum interface. A review article. J.Orthopaedics 6(4),e3-e11.

Kurtz et al., 2007 Kurtz S., Ong K., Lau E., Mowat F., Halpern M., 2007. Projections of primary and revision hip and knee arthroplasty in the United States from 2005 to 2030. J. Bone Joint Surg. Am. 89, 780-785.

Levine et al., 2006 Levine B. R., Sporera S., Poggie R. A., Della Valle C.J., Jacobs J.J., 2006. Experimental and clinical performance of porous tantalum in orthopedic surgery, Biomaterials 27, 4671–4681.

Lewis, 2013 Lewis G., 2013. Properties of open-cell porous metals and alloys for orthopaedic applications, J. Mater. Sci. Mater. Med. 24, 2293-2325.

Liu and Ma, 2004 Liu X., Ma P. X., 2004. Polymeric Scaffolds for Bone Tissue Engineering. Annals of Biomedical Engineering 32 (3), 477-486.

Maccauro et al., 2009 Maccauro G., Iommetti P. R., Muratori F., Raffaelli L., Manicone P. F. and Fabbriciani C., 2009. An Overview about Biomedical Applications of Micron and Nano Size Tantalum, Recent Patents on Biotechnology 3(3), 157-165 .

Maho et al., 2012 Maho A., Linden S. Arnould C., Detriche S., Delhalle J., Mekhalif Z., 2012. Tantalum oxide/carbon nanotubes composite coatings on titanium, and their functionalization with organophosphonic molecular films: A high quality scaffold for hydroxyapatite growth. J. Colloid Interface Sci. 371, 150–158.

Martens et al., 1983 Martens M., Van Audekercke R., Delport P., De Meester P, Mulier J.C. 1983. The mechanical characteristics of cancellous bone at the upper femoral region. J. Biomech. 16, 971-983.

Matsuno et al. 2001 Matsuno H., Yokoyama A., Watari F., Motohiro U., Kawasaki T., 2001. Biocompatibility and osteogenesis of refractory metal implants, titanium, hafnium, niobium, tantalum and rhenium. Biomaterials 22, 1253-1262.

Mediaswanti et al., 2013 Mediaswanti K., Wen C., Ivanova E.P., Berndt C.C., Malherbe F., et al., 2013. A Review on Bioactive Porous Metallic Biomaterials. J. Biomim. Biomater Tissue Eng. 18,104.

Ochiai et al., 2010 Ochiai S., Nakano S., Fukazawa Y., Aly M.S, Okuda H., Kato K., Isobe T., Kita K. and Honma K., 2010. Change of Young‟s Modulus with Increasing Applied Tensile Strain in Open Cell Nickel and Copper Foams. Mater. Trans. 51(5), 925 – 932.

Pflüger et al., 1980 Pflüger G., Plenk H. Jr., Böhler N., Grunschober F., Schider S. 1980. Experimental studies on total knee and hip joint endoprostheses made of tantalum. In: Winter GD, Gibbons DF, Plenk H Jr, eds. Biomaterials. Chichester: John Wiley & Sons, 1982, 161-167.

Rupérez et al., 2012 Rupérez E.; Manero J.M.; Fernández-Fairén M.; Gil F.J.,2012. Método para la obtención de espumas de tántalo para sustitución de tejidos duros. Patent: P201230937, 15/06/2012. Spain.

Ryan et al., 2006 Ryan, G.; Pandit, A.; Apatsidis, 2006. D.P. Fabrication methods of porous metals for use in orthopaedic applications. Biomaterials, 27, 2651–2670.

Sevilla et al., 2007 Sevilla P., Aparicio C., Planell J.A., Gil F.J., 2007. Comparison of the mechanical properties between tantalum and nickel–titanium foams implant materials for bone ingrowth applications. J Alloy Compd. 439, 67–73.

Singh et al., 2010 Singh, R.; Lee, P.D.; Dashwood, R.J.; Lindley, T.C.,2010. Titanium foams for biomedical applications: A review. Mater. Technol. 25, 127–136.

Spoerke and Stupp, 2005 Spoerke E.D., Stupp S.I., 2005. Synthesis of a poly(l-lysine)-calcium phosphate hybrid on titanium surfaces for enhanced bioactivity, Biomaterials 26, 5120-5129.

Torres et al., 2012 Torres Y., Pavón J.J., Rodríguez J.A., 2012. Processing and characterization of porous titanium for implants by using NaCl as space holder. J Mater. Process Tech., 212(5), 1061–1069.

Tuncer et al., 2011 Tuncer, N., Arslan, G., Maire, E., Salvo, L., 2011. Investigation of spacer size effect on architecture and mechanical properties of porous titanium. Mater. Sci. Eng. A 530, 633–642.

Wang et al., 2009 Wang X., Li Y., Xiong J., Hodgson P.D., Wen C., 2009. Porous TiNbZr alloy scaffolds for biomedical applications. Acta Biomater. 5(9),3616-3624.

Wang X et al., 2010 Wang X, Nyman J.S., Dong X. Leng H. Reyes M. Fundamental biomechanics in bone tissue engineering. Chapter 4: Mechanical behaviuor of bone. 2010. Morgan & Clapool Publishers.pp 75-124

Wen et al., 2002 Wen C.E., Yamada Y., Shimojima K., Chino Y., Asahina T., Mabuchi M., 2002. Processing and mechanical properties of autogenous titanium implant materials. J. Mater. Sci.: Mater. Med. 13, 397-401.

Wenjuan et al., 2009 Wenjuan N., Chenguang B., GuiBao Q., Qiang W., 2009. Processing and properties of porous titanium using space holder technique. Mater. Sci. Eng., A 506, 148-151.

Wielding et al., 2015 Wieding J., Lindner T.. Bergschmidt P., Bader R. Biomechanical stability of novel mechanically adapted open-porous titanium scaffolds in metatarsal bone defects of sheep. Biomaterials. Volume 46, April 2015, Pages 35‑47

Wua et al., 2014 Wua S., Liua X., Yeung K.W.K., Liu C., Yang X., 2014. Biomimetic porous scaffolds for bone tissue engineering. Mater. Sci. Eng., : R: Reports 80, 1–36.

Ye and Dunand, 2010 Ye B., Dunand D.C., 2010. Titanium foams produced by solid-state replication of NaCl powders, Mater. Sci. Eng., A 528, 691-697.

Zardiachas et al., 2001 Zardiackas L.D., Parsell D.E., Dillon L.D., Mitchell D.W., Nunnery L.A., Poggie R., 2001. Structure, metallurgy, and mechanical properties of a porous tantalum foam. J. Biomed. Mater. Res. 58(2), 180-187.

Zhou and Zhu, 2013 Zhou Y., Zhu Y., 2013. Three-dimensional Ta foams produced by replication of NaCl space-holders. Mater. Lett. 99, 8–10.

Video

Click here to download Video: video micro_CT (4).avi